引用格式：CHEN Ning, XU Hao, HU Zhengquan, et al. High-sensitivity Fiber-optical Microphone Based on Dual-rib Structure [J]. Acta Photonica Sinica, 2026, 55(2):0206001
陈宁,徐浩,胡政权,等.高灵敏双重肋结构光学麦克风研究[J].光子学报,2026,55(2):0206001

高灵敏双重肋结构光学麦克风研究

陈宁[1],徐浩[1],胡政权[1],尧耀文[1],张琦[1],黄怿[1],邵剑[2],李群[2],
张小贝[1],王廷云[1]
(1 上海大学 特种光纤与光接入网重点实验室,上海 200444)
(2 国网江苏省电力有限公司电力科学研究院,南京 211103)

摘 要:设计并制备了一种新型双重肋结构的高灵敏度光学麦克风,该传感单元由双重肋结构膜片、单模光纤与石英套筒构成。基于有限元仿真优化肋结构参数,并使用皮秒激光微纳加工技术实现双重肋结构膜片的制备。所研制的光学麦克风在15.58 kHz下实现了1 418.9 mV/Pa的高灵敏度和61.17 dB的信噪比,展现出优越的声信号获取能力、高灵敏传感特性和良好的方向性。该光学麦克风有望应用于电力传感领域,为电力运行设备的微弱声信号探测、局部放电检测、设备故障诊断与线路在线监测提供保障。

关键词:光学麦克风;光纤传感器;双重肋结构;激光微纳加工技术;光纤传感技术
中图分类号:TN253 **文献标识码**:A **doi**:10.3788/gzxb20265502.0206001

0 引言

声学信号的精确探测在国防安全、地震监测、工业无损检测、生物医学诊断等领域具有广泛而重要的应用。声传感器主要包括电学型与光学型两大类。电学声传感器如驻极体麦克风和电容式麦克风,因工艺成熟和体积小而得到广泛应用,但其在电磁干扰环境、高温环境以及长距离传输中往往存在信号衰减、抗干扰能力不足的问题[1]。相比之下,光学麦克风凭借其绝缘性、抗电磁干扰能力强、可远距离传输以及体积微小等优势,逐渐成为声学探测领域的重要发展方向。

近年来,光学麦克风在灵敏度和频响特性方面取得了长足进展,常见的干涉式[2-4]、布拉格光栅式[5]以及微腔耦合式[6]的光学麦克风在声学探测中展现出良好性能。其中非本征法珀干涉式光学麦克风因其结构紧凑,易于制备等优点被广泛研究[7]。通常,非本征法珀结构由光纤端面和传感膜片构成。目前膜片的研究主要聚焦于材料种类和结构设计。材料属性和结构设计对膜片的机械特性和振动响应都有显著影响,因此膜片材料选择和结构设计都是光学麦克风研究的重点。常见的膜片材料包括硅、高分子聚合物、石墨烯以及金属等。国内外已有大量关于膜片材料的研究,2013年斯坦福大学WONUK J等[8]通过毛细玻璃管将硅光子晶体膜片与单模光纤耦合,提升了振动响应和位移灵敏度。2020年华中科技大学ZHANG Wei等[9]利用金膜片作为反射端面,制成一种紧凑型传感器,频率响应覆盖20~150 kHz,信噪比达48 dB。2021年海南大学LI Long等[10]采用PDMS薄膜,频率响应范围扩展至430 kHz,信噪比达70 dB。这类传感器虽具高灵敏度和良好频率响应,但受限于材料要求和复杂工艺。相比之下,石英玻璃凭借其优异的机械稳定性、较低的热膨胀系数和优良的光学性能,通过合理的结构设计,可以有效提升传感器的灵敏度。因此,结合石英材料的优势与高灵敏度的设计,能够显著优化传感器性能。

在结构方面,通过优化膜片结构设计,可以改变受力方式或传递路径,在相同声压下获得更大的变形,

基金项目:国家重点研发计划(2022YFF0708400)
第一作者:陈宁,chenning9707@163.com
通讯作者:张小贝,xbzhang@shu.edu.cn
收稿日期:2025-09-08;**录用日期**:2025-10-18

从而显著提高传感器的灵敏度和响应性能。2017年美国克莱姆森大学LIU Jie等[11]利用激光微加工技术，在硅膜上制备了微尺度悬臂梁，传感器谐振频率为0.74 MHz，灵敏度9.75 μm/MPa，其谐振频率高但低频响应受限。2021年西北工业大学LI Haoyong等[12]采用梁支撑结构，拓宽了频率响应范围，并在前端加装菲涅尔波带片，使灵敏度提升至239.88 mV/Pa，但该设计工艺复杂、器件尺寸较大。2023年上海大学ZHANG Lina等[13]利用MEMS工艺在硅片上引入沟槽结构，使声压响应较传统圆形振膜提升约5倍，在40 kHz时灵敏度为20.08 mV/Pa，在61.50 kHz谐振点达到172.42 mV/Pa，但整体灵敏度仍需进一步提升。

本文提出了一种基于双重肋结构的光学麦克风。该方案通过在圆环之间引入肋条，在保持膜片边缘刚度的同时显著降低有效质量，提高灵敏度。此外，本文采用皮秒激光微纳加工工艺在石英基底上实现石英膜片的制备。所制备的光学麦克风具有高灵敏度、高信噪比和良好方向性，为光学麦克风在电力检测和声源定位等应用提供了新的解决方案。

1 传感器设计和制备

1.1 结构设计

如图1(a)所示，该光学麦克风主要由双重肋结构膜片、玻璃套筒和单模光纤组成。其中，双重肋结构如图1(b)所示，中心为圆形膜片，圆环之间为肋条。单模光纤被插入套筒中，光纤端面作为第一反射面并与膜片内表面构成法珀腔。肋结构膜片的材料为熔融石英，通过皮秒激光制备，并组装于玻璃套筒的表面。当声压作用于肋结构膜片上时，膜片在声信号作用下产生形变，导致法珀腔的腔长改变，进而导致干涉光强改变，通过光电转换器将光信号转化为电信号，从而实现声波检测。

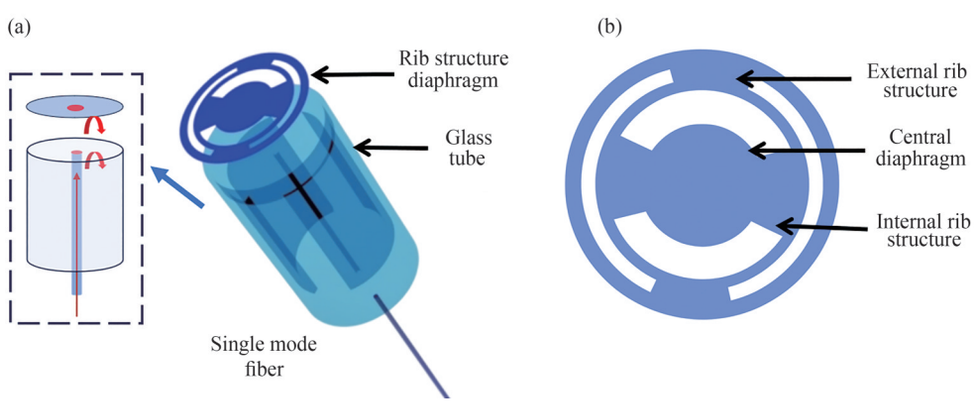


图1 传感器结构示意图及光路图。(a)所提出传感器结构示意图；(b)肋结构光纤声传感器示意图

Fig. 1 Schematic diagram of the sensor structure and optical path. (a) Schematic diagram of the proposed sensor structure; (b) Schematic diagram of the ribbed fiber optic acoustic sensor.

为了优化膜片的参数，首先对圆形膜片振动理论进行分析。传感膜的尺寸和材料决定了传感器的灵敏度和谐振频率。当声波施加到圆形膜片上时，圆形膜片会产生微弱的变形。四周固定约束的膜片中心位移d为[14]

$$d=\frac{3(1-\nu^2)Pr^4}{16Et^3} \tag{1}$$

式中，υ和E分别是圆形膜片材料的泊松比和杨氏模量，P是施加在圆形膜片上的压力，r和t分别是圆形膜片的半径和厚度。膜片的中心位移和谐振频率均与材料属性和膜片尺寸有关。其一阶谐振频率f可以表示为[15]

$$f=\frac{10.21t}{2\pi r^2}\sqrt{\frac{E}{12\rho(1-\nu^2)}} \tag{2}$$

式中，ρ是膜片材料的密度。当膜片厚度增加时，谐振频率升高；而当膜片半径增大时，谐振频率降低。此外，膜片的灵敏度不仅与其性质有关，还与外部声信号频率有关。膜片在声信号下的动态灵敏度为[16]

$$S_{\mathrm{d}}=\frac{d}{P}=\frac{3(1-\nu^2)r^4}{16Et^3}=\frac{1}{\sqrt{\left(1-\frac{f_{\mathrm{m}}^2}{f_{\mathrm{c}}^2}\right)^2+4\zeta^2\left(\frac{f_{\mathrm{m}}}{f_{\mathrm{c}}}\right)^2}} \tag{3}$$

式中，f_{c}是膜片的谐振频率，f_{m}是外部声信号的频率，ζ是振动的阻尼比。随着阻尼比的减小，膜片的灵敏度增强，因此通过改变形状和结构可以获得更强的声压响应[17]。根据式(3)，当f_{c}等于f_{m}时，振动的阻尼比ζ非常小，此时膜片的动态灵敏度达到最大。因此，减少膜片振动造成的阻尼，可以提升结构的灵敏度。在双重肋结构膜片中，降低阻尼是通过优化肋条的数量和位置实现的[18-19]。

根据上述理论模型，采用COMSOL Multiphysics固体力学模块，对双重肋结构膜片的振动特性进行有限元仿真分析，石英材料参数为$\rho=2\ 650\ \mathrm{kg/m^3}$，$E=72\ \mathrm{GPa}$，$v=0.14$。中心圆形膜片的半径$r$设为2.2 mm，内外部肋结构弧度为60°，将最外侧套筒设置为固定约束。首先研究肋数量对谐振频率和灵敏度的影响，仿真结果如图2所示，肋数量的增加显著增大了膜的谐振频率，但同时降低了灵敏度。这是因为随着肋的数量增加，膜片的刚性和振动模态发生变化，更多的肋条分散了外部激励的能量。

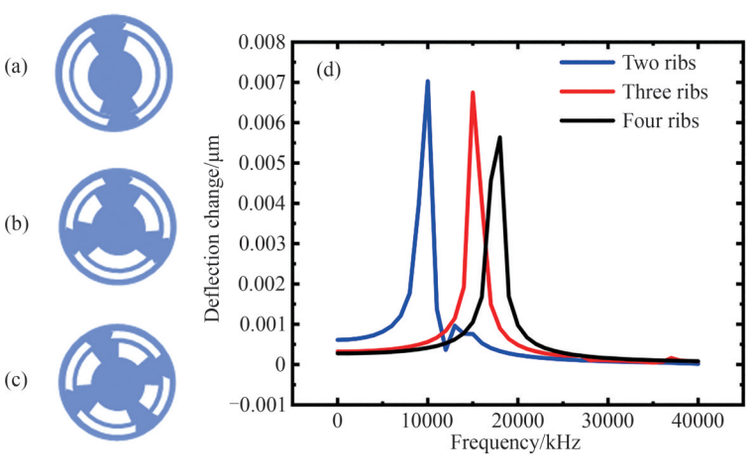


图2　不同个数的肋结构仿真结果。(a)(b)(c)分别为双肋结构，三肋结构和四肋结构；(d)为不同肋结构数量的仿真结果

Fig. 2　Simulation Results of Rib Structures with Various Counts. (a), (b), and (c) represent double-ribbed, triple-ribbed, and quadruple-ribbed structures, respectively; (d) shows the simulation results for different numbers of ribs.

进一步分析了内外部肋结构位置和整体膜片的厚度对灵敏度的影响，仿真结果如图3(a)所示，90°交叉分布的肋结构灵敏度较同一直线分布的肋结构形变量提升了1个数量级。这是由于内外部肋结构交叉配置有助于通过相互耦合作用优化膜片的振动模式。整体厚度对灵敏度的影响如图3(b)所示，随着厚度的减

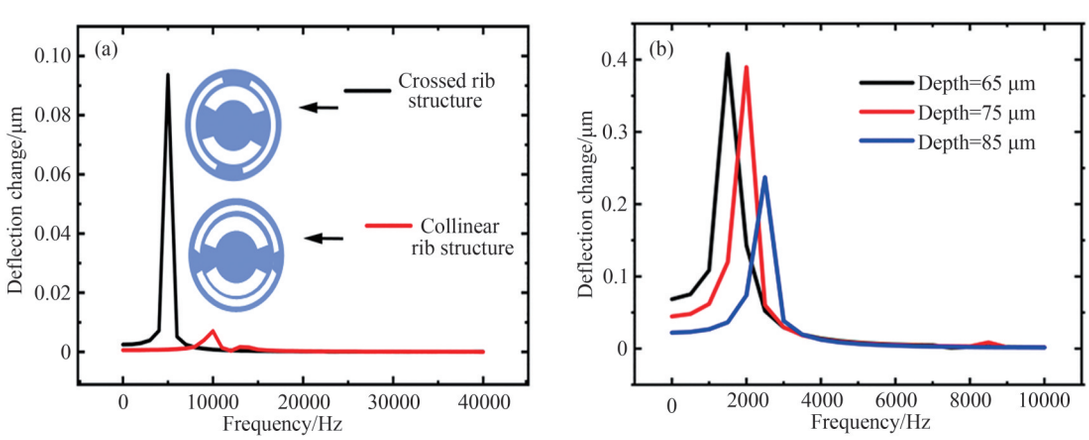


图3　不同位置肋结构和不同厚度膜片的仿真结果。(a)不同位置肋结构仿真结果；(b)不同厚度膜片的仿真结果

Fig. 3　Simulation results of rib structures at different positions and different depth of diaphragm. (a) Simulation results of rib structures at different locations; (b) Simulation results of diaphragms with different thicknesses.

小，灵敏度逐渐增大。考虑到加工工艺，为制备出形变量较大的膜片，本文选择双重交叉肋结构，膜片的厚度设置为65 μm，总体直径为10 mm。

1.2 传感器的制备

图4是用于制备双重肋结构膜片的皮秒激光微纳加工系统。该系统通过超快激光与精密三维位移平台精确控制传感膜片的加工过程，从而实现高精度的结构制造。皮秒激光微纳加工系统通过发射脉冲宽度在皮秒级别的激光束，能够在极短的时间内对材料进行局部加热和材料去除。因此，在光学麦克风的膜片结构制作过程中，皮秒激光可以高效、精确地制造出复杂的双重肋结构，同时保证膜片的机械强度和稳定性。为了提高加工的精度，在加工之前还需要对激光扫描的路径进行优化，这是因为在实际激光微纳加工过程中，若完全依赖原始设计结构进行路径规划，往往会导致加工过程耗时较长，且由于激光束在连续扫描过程中产生的热量累积，势必在结构边缘区域引发热损失或形变。激光加工的功率由软件控制，加工过程中使用的物镜是数值孔径为0.4的20倍物镜，激光功率为10 mW，激光扫描速度1.0 mm/s，在加工完成后，在膜片的内表面镀一层金膜，以提高反射率。图5(a)展示了其加工后的在显微镜下观察的实物图，膜片厚度为65.07 μm，膜片直径为10.05 mm。可以清晰观察到膜片表面的双重肋状结构分布均匀且轮廓清晰，表明该技术能够在微纳尺度下实现高精度的结构制造。并且所采用的皮秒激光微纳加工工艺具有超短脉宽、热影响区小和加工精度高等优势，可在全石英体系上稳定实现双重肋结构膜片的高效制备。对不同样品的检测结果表明，肋宽度一致性小于±2.0 μm，腔长偏差小于±1.5 μm，表面粗糙度约为70-80 nm。结合能量监测以及加工后的光学检测，这些结果表明该工艺能够实现稳定可控的批量制备，并保证器件在结构尺寸和表面质量上的高度一致性。

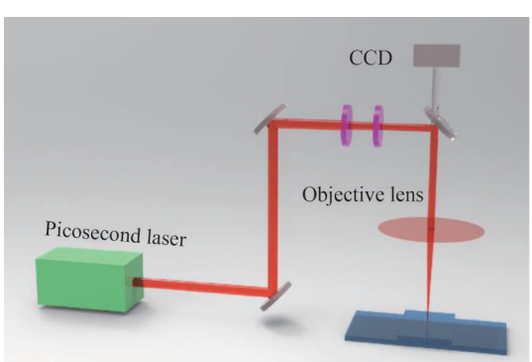


图4 皮秒激光微纳加工系统

Fig. 4 Schematic diagram of laser micro-nano machining system

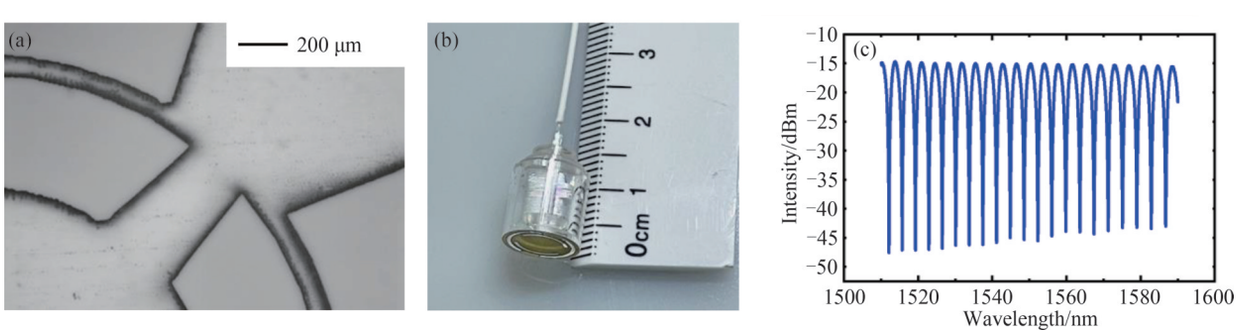


图5 传感器的实物图和反射光谱图。(a)双重肋结构实物图；(b)传感器组件图；(c)反射光谱图

Fig. 5 Photograph of the sensor and its reflection spectrum. (a) Schematic diagram of dual-rib structure diagram; (b) Sensor assembly diagram; (c) Reflection spectrum

在完成膜片制备后，对传感器进行组装。主要包括以下四个步骤：1)去除单模光纤涂覆层，并实现端面切割。为保证单模光纤与石英套筒粘结，并与双重肋结构膜片共同形成稳定的法珀腔，需对光纤末端进行预处理。通过使用高精度切割刀切割端面，确保其平整且垂直于光纤轴线；2)单模光纤与毛细管的粘接。

将光纤插入外径1 mm，内径0.3 mm的玻璃管中，并通过光纤光栅解调仪（SM125，Micron Optics）实时观察光谱，防止光纤端面损坏；3）膜片与石英套筒的粘接。将镀有金膜的反射面与涂有UV胶的内径9 mm，外径10 mm的石英套筒固化；4）将光纤插入固化好的套筒中，并通过光纤光栅解调仪实时测量腔长和光谱，确保有较高的对比度。组装后的实物图如图5（b）所示，反射光谱如图5（c）所示，对比度超过30 dB，表明传感器有良好的光学性能。

2 传感器的测试

为实现传感器的性能表征，搭建了声学测试的实验装置如图6所示。采用可调谐激光器（TSL-710，Santec）作为光源，其波长通过软件控制面板进行精确控制。激光输出通过光学环形器（6015-3-APC，Thorlabs）耦合至传感器。传感器反射的信号由光电探测器（PDA50B2，Thorlabs）接收，并通过示波器（MSO44，Tektronix）做进一步分析。声波由压电换能器（PZT）激发，该换能器由信号发生器（DG1062，Rigol）驱动，并通过电压放大器（ATA-2041，Aigtek）放大。校准后的电容式麦克风（4939-A-011，B&K）被放置在待测传感器附近，用于测量声压并作为参考。

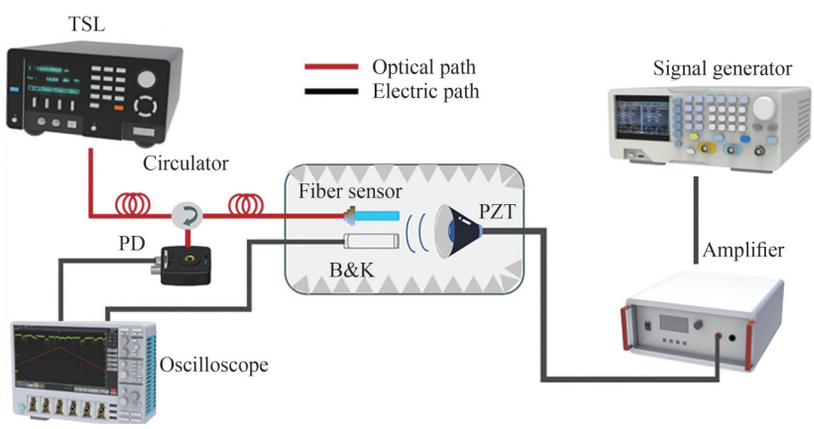


图6 声学测试实验装置图

Fig. 6 Schematic diagram of the acoustic testing system

图7为制备的光学麦克风时域信号及其对应的信噪比（Signal Noise Ratio，SNR）测试结果。图7（a）～（c）展示了传感器在频率分别为10.00 kHz、15.58 kHz和20.00 kHz下的时域响应，相应的输出电压信号幅值分别为48.90 mV、350.40 mV和18.30 mV。图7（d）～（f）为三种信号对应的傅里叶变换结果，信噪比分别为63.24 dB、61.17 dB和50.70 dB。表明该光学麦克风能够实现高灵敏度和低噪声的声信号检测。

图8展示了所制备光学麦克风的灵敏度与频响测试结果。图8（a）为输出电压与声压之间的关系，图8（b）为电压幅值随频率变化的分布。可以看出，光学麦克风的输出电压与声压呈现出线性关系。实验数据（黑色圆点）与线性拟合曲线（红色直线）吻合良好，拟合结果为$y=1\ 418.9x+57.327$，灵敏度达到最大值约为1 418.9 mV/Pa，拟合系数$R^2=0.996$，表明该麦克风在该频率范围内具备高线性响应。图8（b）展示了光学麦克风的频响特性曲线。在15.58 kHz附近，表明该频率点为光学麦克风的主要工作频率点。其他频段的灵敏度较低，呈现出典型的频率选择性响应特性。该灵敏度数据表明，光学麦克风在15.5 kHz的频率下具有显著的高灵敏度响应，并且在该频段具备优异的声压响应能力。

方向性也是声传感器的重要指标。在方向性实验中，将图6中的传感器固定，声源在固定半径下，设置步长为30°，从0°到360°旋转，并记录每一个角度下的时域波形。将传感器检测到的归一化电压信号和角度的关系以极坐标的形式呈现，如图9所示。实验结果表明所提出的双重肋结构声传感器具有良好的方向性，这在传感器的应用中是非常重要的。

将所设计的传感器与其他已报道的传感器相比较，如表1所示。可见，该传感器与表1中文献的结果如凹槽形、波纹及梁支撑等膜片结构相比，灵敏度高3～4倍，同时保持了相同水平的信噪比。此外，所用的二

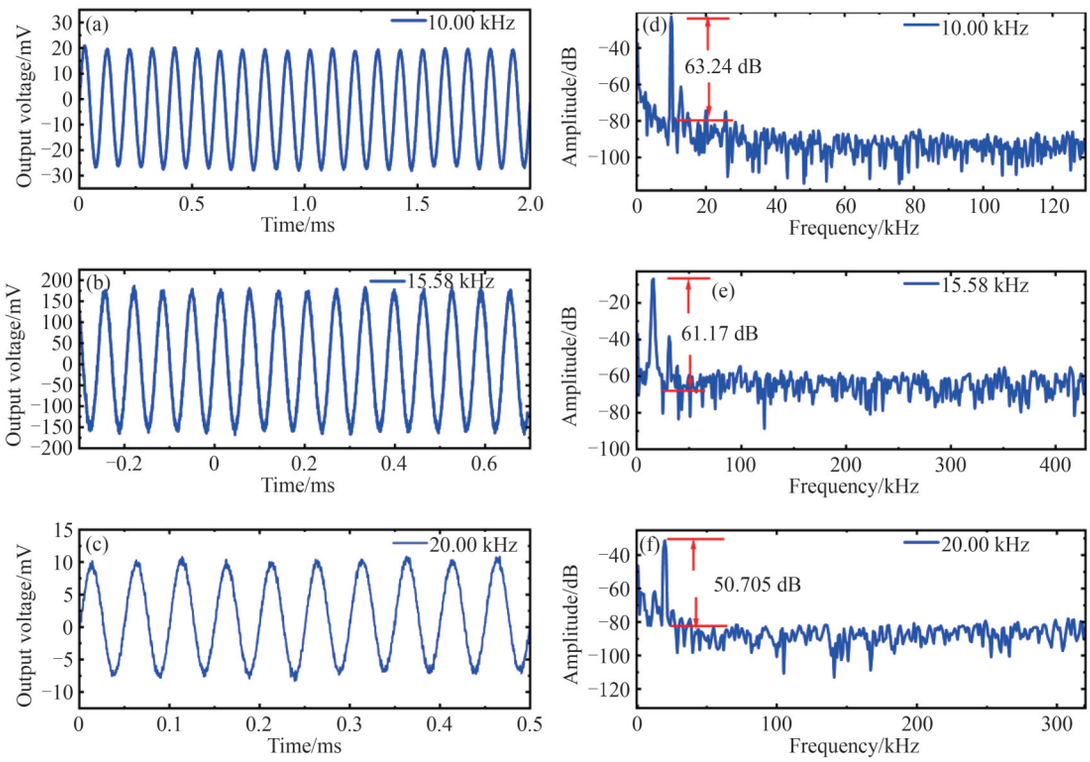


图7 传感器检测到的时域响应及频域响应图。(a)(b)(c)分别为10.00 kHz,15.58 kHz和20.00 kHz的时域响应;(d)(e)(f)分别为10.00 kHz,15.58 kHz和20.00 kHz对应的频率响应

Fig.7 Time-domain and frequency-domain responses of proposed sensor. (a), (b), and (c) are the time-domain responses at 10.00 kHz, 15.58 kHz, and 20.00 kHz, respectively; (d), (e), and (f) are the frequency responses at 10.00 kHz, 15.58 kHz, and 20.00 kHz, respectively

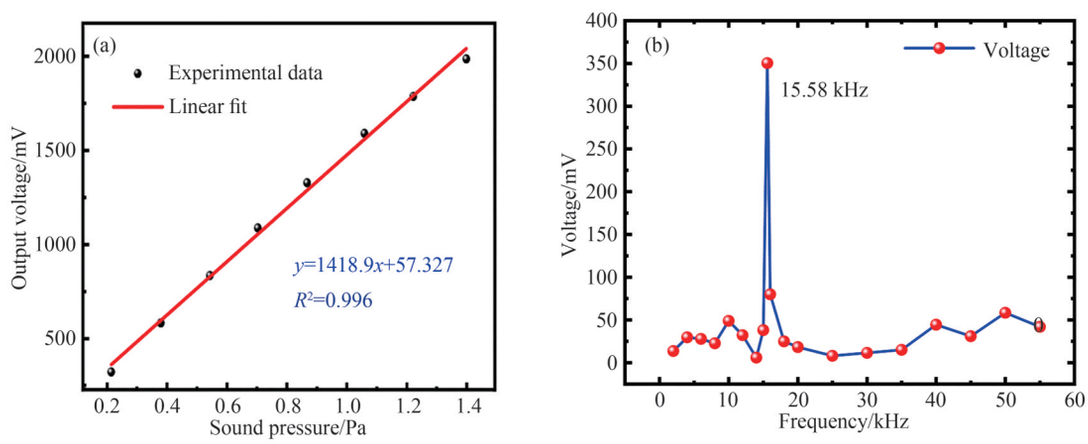


图8 传感器灵敏度与频响测试结果。(a)传感器灵敏度特性;(b)频率响应特性

Fig. 8 Test results of sensor sensitivity and frequency response. (a) Sensitivity characteristic of the sensor; (b) Characteristic of frequency response

氧化硅材料温度稳定性强,有助于应用于极端环境。文献[21]中使用的氧化石墨烯薄膜制备过程相对繁琐。因此,本文所提出的基于双重肋结构的光纤声传感器具有高灵敏,加工简单等优点。需要指出的是,传感器在实际应用中仍会受到不同场景干扰因素的影响。例如,电力监测中的强电磁与机械振动、石化环境中的背景噪声与气流扰动,以及高温辐照等极端条件,均可能导致灵敏度下降或信号漂移。针对这些问题,可依托光纤传感的抗电磁干扰特性,并结合减振温度补偿等封装设计加以改善,从而提升器件在复杂环境下的稳定性与可靠性。

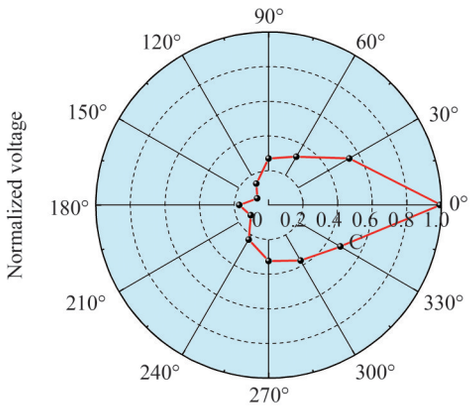


图9　传感器的方向性测试

Fig. 9　Directional property test of proposed sensor

表1　不同特性传感器对比

Table 1　Comparison of sensors with different characteristics

Structure	Material	Sensitivity	SNR	Reference
Grooved	Silicon	172.42 mV/Pa	64 dB@60 kHz	[13]
/	Sapphire	13.58 mV/Pa	/	[20]
Corrugated	Graphene-oxide	299.42 mV/Pa	76.66 dB@1 kHz	[21]
Beam-supported	Silicon	251 μPa/Hz$^{1/2}$	52 dB@30 kHz	[22]
Outer-ring clover	Silica	1 362 nm/kPa	67 dB@300 kHz	[23]
Drumstick-shaped cantilever	stainless steel	302.8 mV/Pa	78.6 dB@1 kHz	[24]
Rib structure	**Fused silica**	**1 418.9 mV/Pa**	**60.47 dB@30 kHz**	**This work**

3　结论

本文设计并制备了一种基于双重肋结构的光学麦克风。实验结果表明，双重肋结构能够显著提升膜片在声波作用下的形变量，有效改善传感器的声—机械形变转化效率。而皮秒激光微纳加工的全石英结构则确保了器件的性能一致性及在复杂环境下的长期可靠性。基于此，所研制的传感器在15.58 kHz下实现了1 418.9 mV/Pa的超高灵敏度，同时信噪比达61.17 dB，表现出优异的声学探测能力。性能优于多种现有膜片结构，并在信噪比上保持良好水平。此外，传感器在具备良好方向性的同时，也展现了在强电磁、振动及噪声等复杂干扰下的稳定监测潜力。这些优势使其不仅能满足极端电力监测的苛刻要求，更在医疗、石化及国防等广阔领域拥有巨大的应用潜力。

参考文献

[1] GAO Chunming, NIE Feng, ZHANG Ping, et al. Optical fiber acoustic sensors[J]. Opto-Electronic Engineering, 2018, 45(9): 190050.
高椿明, 聂峰, 张萍, 等. 光纤声传感器综述[J]. 光电工程, 2018, 45(9): 180050.

[2] DUQUE W S, RODRíGUEZ DíAZ C A, LEAL-JUNIOR A G, et al. Fiber-optic hydrophone based on Michelson's interferometer with active stabilization for liquid volume measurement[J]. Sensors, 2022, 22(12): 4404.

[3] ZHAO Xinyu, MA Fengxiang, WANG Zhengzhi, et al. Multicomponent trace gas detection technology based on fiber optic photoacoustic sensing[J]. Acta Photonica Sinica, 2024, 53(3): 0306001.
赵新瑜, 马凤翔, 王正之, 等. 基于光纤光声传感的多组分痕量气体检测技术[J]. 光子学报, 2024, 53(3): 0306001.

[4] LI Liu, LU Ping, LIAO Hao, et al. Fiber-optic michelson interferometric acoustic sensor based on a PP/PET diaphragm [J]. IEEE Sensors Journal, 2016, 16(9): 3054-3058.

[5] ZHANG Pengfei, XIANG Ziyang, WANG Fangjun, et al. Fiber optic acoustic sensor based on fiber Bragg grating Fabry-Perot (FBG-FP) cavity[C]. 2021 19th International Conference on Optical Communications and Networks (ICOCN), IEEE, 2021: 1-3.

[6] GUGGENHEIM J A, LI Jing, ALLEN T J, et al. Ultrasensitive plano-concave optical microresonators for ultrasound sensing[J]. Nature Photonics, 2017, 11(11): 714-719.

[7] HUANG Yuhao, REN Qianyu, WANG Jun, et al. Three-wavelength small-signal calibration method for Fabry-Perot

sensors based on Lissajous curve fitting[J]. Acta Photonica Sinica, 2025, 54(6): 0606001.
黄宇浩,任乾钰,王军,等. 基于Lissajous曲线拟合的Fabry-Perot传感器三波长小信号标定方法[J]. 光子学报, 2025, 54(6):0606001.
[8] JO W, AKKAYA O, SOLGAARD O, et al. Miniature fiber acoustic sensors using a photonic-crystal membrane[J]. Optical Fiber Technology, 2013, 19(6): 785-792.
[9] ZHANG Wei, LU Ping, NI Wenjun, et al. Gold-diaphragm based Fabry-Perot ultrasonic sensor for partial discharge detection and localization[J]. IEEE Photonics Journal, 2020, 12(3): 1-12.
[10] LI Long, WANG Jun, WANG Wei, et al. Polydimethylsiloxane diaphragm-based fiber ultrasonic sensor with high sensitivity and wide spectrum response range[J]. AIP Advances, 2021, 11(7):075021.
[11] LIU Jie, YUAN Lei, LEI Jincheng, et al. Micro-cantilever-based fiber optic hydrophone fabricated by a femtosecond laser [J]. Optics Letters, 2017, 42(13): 2459-2462.
[12] LI Haoyong, BU Jian, LI Wenli, et al. Fiber optic Fabry-Perot sensor that can amplify ultrasonic wave for an enhanced partial discharge detection[J]. Scientific Reports, 2021, 11(1): 8661.
[13] ZHANG Lina, HUANG Yi, NIU Xiling, et al. High-sensitivity fiber optic Fabry-Perot ultrasonic sensor based on a grooved silicon diaphragm for partial discharge detection[J]. Applied Optics, 2023, 62(25): 6809-6815.
[14] ZHAO Shuang, JIANG Yi, DENG Hui, et al. High sensitivity all-sapphire fiber diaphragm-based extrinsic Fabry-Perot interferometric pressure sensor for ultra-high temperature environments[J]. Optics Express, 2025, 33(18): 37322-37333.
[15] ZHANG Qi, LEI Jincheng, CHEN Yizhen, et al. 3D printing of all-glass fiber-optic pressure sensor for high temperature applications[J]. IEEE Sensors Journal, 2019, 19(23): 11242-11246.
[16] CHEN Jian, RAO Jing, LISEVYCH D, et al. Broadband ultrasonic focusing in water with an ultra-compact metasurface lens[J]. Applied Physics Letters, 2019, 114(10): 104101.
[17] YOU Zhiwei, GAN Jinghang, YANG Chong, et al. Piezoelectric MEMS microphones based on rib structures and single crystal PZT thin film. Microsystems & Nanoengineering, 2024, 10(1): 167.
[18] YAO Mian, ZHANG Yangxi, OUYANG Xia, et al. Ultracompact optical fiber acoustic sensors based on a fiber-top spirally-suspended optomechanical microresonator[J]. Optics Letters, 2020, 45(13): 3516-3519.
[19] WANG Wenhua, YU Qingxu, JIANG Xinsheng. High sensitivity diaphragm based extrinsic Fabry-Pérot interferometric optical fiber underwater ultrasonic sensor[J]. Optoelectronics and Advanced Materials-Rapid Communications, 2012, 6(7): 697-702.
[20] WANG Jiayan, LI Huayang, TANG Luhong, et al. Au-Au bonding-associated lapping and polishing technique for sapphire-based Fabry-Perot acoustic sensor applied for harsh environment[J]. IEEE Sensors Journal, 2022, 22(19): 18454-18462.
[21] LIU Yang, LI Cheng, YU Lingxiao, et al. Ultra-high sensitivity fiber optic microphone with corrugated graphene-oxide diaphragm for voice recognition[J]. Nano Research, 2024, 17(8): 7593-7602.
[22] LI Haoyong, LV Jiaming, LI Delin, et al. MEMS-on-fiber ultrasonic sensor with two resonant frequencies for partial discharges detection[J]. Optics Express, 2020, 28(12), 18431-18439.
[23] WEN Jialin, YANG Tingyun, ZHENG Zeyu, et al. Two-photon 3D-printed fabry-pérot interferometric sensor for ultrasensitive high-frequency ultrasonic detection[J]. Journal of Lightwave Technol, 2025, 43(2): 948-956.
[24] TIAN Shen, CHEN Pengbo, JIAO Mingqi, et al. Geometry optimization of cantilever-based optical microphones[J]. Optics Letters, 2024,49(8): 2101-2104.

High-sensitivity Fiber-optical Microphone Based on Dual-rib Structure

CHEN Ning[1], XU Hao[1], HU Zhengquan[1], YAO Yaowen[1], ZHANG Qi[1], HUANG Yi[1], SHAO Jian[2], LI Qun[2], ZHANG Xiaobei[1], WANG Tingyun[1]

(1 *Key Laboratory of Specialty Fiber Optics and Optical Access Networks, Shanghai University, Shanghai* 200444, *China*)
(2 *Electric Power Research Institute of State Grid Jiangsu Electric Power Co., Ltd, Nanjing* 211103, *China*)

Abstract: Fiber-optic microphones have emerged as an innovative solution in the field of acoustic sensing due to their compact size, excellent immunity to electromagnetic interference, and superior insulation performance. These attributes make them ideal for use in various challenging environments such as power systems, healthcare, petrochemical industries, and national defense. However, despite these advantages, traditional fiber-optic microphones still face challenges in terms of sensitivity, stability, and insulation,

particularly in high-performance or demanding conditions. Some existing designs struggle with low sensitivity in detecting weak acoustic signals or may experience degradation in performance due to material instability and electromagnetic interference under extreme conditions. Additionally, ensuring stable insulation properties in high-temperature or harsh electromagnetic environments remains a challenge for many fiber-optic microphone designs. Therefore, this work proposes and fabricates a novel high-sensitivity fiber-optic microphone featuring a dual-rib diaphragm structure.

The microphone unit consists primarily of a dual-rib diaphragm, a single-mode optical fiber, and a glass sleeve, which work in synergy to convert acoustic signals into optical signals for high-precision measurement. The diaphragm′s design was optimized through finite element simulations to achieve the desired resonance characteristics and enhance its acoustic sensitivity. Specifically, the ribbed diaphragm structure was designed to increase its flexibility, thereby improving its response sensitivity to pressure changes. To fabricate the diaphragm, we employed a picosecond laser micro-nano machining system, which allowed us to achieve high precision and fine features in the diaphragm′s ribbed structure. This fabrication process ensures that the diaphragm can withstand mechanical stresses during acoustic signal detection while maintaining high sensitivity.

The fabricated fiber-optic microphone exhibits a high sensitivity of 1 418.9 mV/Pa and a signal-to-noise ratio of 60.47 dB at a resonance frequency of 15.58 kHz, demonstrating excellent performance in acoustic signal acquisition. The microphone′s high sensitivity makes it suitable for detecting weak acoustic signals, even in environments with significant background noise. Moreover, the microphone displays a strong directional response, which is critical for applications that require precise localization of sound sources. These characteristics make it an excellent candidate for use in a variety of industrial and scientific applications, where accurate and reliable sound detection is required.

The potential applications of this high-sensitivity fiber-optic microphone are vast. It is particularly suited for power sensing, where it can be used to detect weak acoustic signals from power equipment, monitor partial discharges, diagnose faults, and enable online monitoring of power lines. The microphone′s immunity to electromagnetic interference and high sensitivity make it ideal for use in environments with high levels of electrical noise. In addition, the microphone′s ability to detect low-level acoustic signals makes it a promising tool for applications in healthcare, such as monitoring bodily sounds, as well as in the petrochemical industry for detecting gas leaks and machinery failures. Beyond these initial applications, the fiber-optic microphone holds promise for many other emerging fields. For example, it could be integrated into advanced monitoring systems for industrial automation, where real-time acoustic feedback is used for predictive maintenance and early detection of mechanical failures. In the field of robotics, the microphone′s small size and high sensitivity could be leveraged in autonomous systems for environmental sound detection and localization. Additionally, as wireless technology continues to advance, fiber-optic microphones could be used in conjunction with wireless communication systems for remote sensing applications, further extending their potential. Future research will focus on optimizing the diaphragm design to achieve a broader frequency response and enhancing the microphone′s robustness in extreme environments. Additionally, efforts will be directed at improving the signal processing capabilities of the fiber-optic microphone to ensure high-performance operation in complex and diverse environments. This work lays a solid foundation for the development of high-sensitivity fiber-optic microphones, which will undoubtedly lead to their widespread application in high-performance acoustic sensing fields, offering substantial benefits for industrial, scientific, and healthcare applications.

Key words: Fiber-optic microphone; Optic fiber sensor; Dual-rib structure; Laser micro/nano machining; Optical fiber sensing technology

OCIS Codes: 060.2370; 120.2230; 060.2300; 120.4210

CSTR: 32255.14.gzxb20265502.0206001

Foundation item: National Key Research and Development Program of China (2022YFF0708400)